Description of polarons in ceria using Density Functional Theory

2014 J. Phys.: Conf. Ser. 526 012002

(http://iopscience.iop.org/1742-6596/526/1/012002)

Journal of Physics: Conference Series **526** (2014) 012002 doi:10.1088/1742-6596/526/1/012002

Description of polarons in ceria using Density Functional Theory.

Christopher WM Castleton and Amy L. Lee
School of Science and Technology, Nottingham Trent University, NG11 8NS, UK
E-mail: Christopher.Castleton@ntu.ac.uk

Jolla Kullgren and Kersti Hermansson
Department of Chemistry, Uppsala University, Box 538, Uppsala, Sweden

Abstract. The performance of various density functional theory (DFT) functionals in reproducing the localization of Ce*4f* electrons to form polarons in cerium dioxide (ceria) is studied. It is found that LDA+U with U=6 eV provides the best description, followed by GGA+U with U=5 eV. Hybrids perform worse, with PBE0 better than HSE06 and HSE03. It is also demonstrated that the improvement in the description of the polarons obtained from LDA+U and GGA+U is due primarily to the effect the U has on the *filled* Ce*4f* states, but the improvement obtained using the hybrids is primarily due to their effect on the *empty* states. This difference can be expected to strongly impact some detailed predictions for the properties of ceria obtained using the two classes of functional.

1. Introduction

The wide bandgap material cerium dioxide (ceria, CeO_2,) has applications in fuel cells, gas sensors and catalysis, but has proved a challenge for theoretical studies. It has an O*2p* based valence band and a nominal Ce*5d* based conduction band, see Fig 1, but in between lies a narrow, empty band of Ce*4f* states. Any potential conduction electron added via doping or defect creation enters this band and localizes onto a single Ce site, breaking the crystal's translational symmetry and inducing a local lattice distortion around the Ce site in question. This forms a "polaron", ie a self-trapped electron, Ce_{Ce}^{-1}, with an energy gain of roughly 1eV. Polarons generally form coupled to other defects, such as Rh adatoms [2] or oxygen vacancies. Oxygen ions have a formal charge of -2, so removing a neutral oxygen (as part of an oxygen molecule) necessarily leaves behind a +2 charged vacancy $V_O^{+2}$and two electrons, which in ceria both form polarons. These three remain electrostatically bound in a neutral $\left[V_O^{+2} - 2Ce_{Ce}^{-1}\right]$ complex, which can adopt a wide range of configurations [5]. Conductivity studies [3] have shown that these polarons are well described by the "Small Polaron Model" of Holstein [4], meaning that the radius of the localized charge and lattice distortion are on the order of one lattice spacing. This is also supported by scanning tunnelling microscopy (STM) images of vacancies and vacancy clusters [1], which are best understood if the two electrons are indeed localized in Ce*4f* states on specific Ce ions.

Obtaining a localized description of these Ce_{Ce}^{-1} polarons using Density Functional Theory (DFT) is hard, requiring the use of either LDA+U, GGA+U, [7, 8, 9] or hybrid functionals

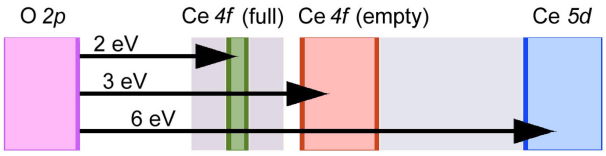

Figure 1. Schematic band diagram for ceria, showing the O*2p* based valence band, and empty Ce*5d* and Ce*4f* bands, plus the filled, localized (polaronic) Ce*4f* states.

[6, 9]. The performance of these in describing the bulk properties (structures, bandgaps etc) of ceria and the sesquioxide, Ce_2O_3, as well as $\left[V_O^{+2} - 2Ce_{Ce}^{-1}\right]$ complexes has been assessed [6, 7, 8, 9]. The best description is obtained using LDA+U with $U = 6$ eV. The hybrids produce qualitatively reasonable descriptions, but are not as good quantitatively. For example, B3LYP does reasonably well for the electronic properties but not for the structure, while PBE0 does well for the structure but not for the bandgaps.

While numerous DFT studies have examined polarons associated with $\left[V_O^{+2} - 2Ce_{Ce}^{-1}\right]$ and other defects, only a few have considered the properties of isolated polarons [10], and we are not aware of any assessment of the quality of the description of lone polarons obtained using different functionals. So we will here compare the description of lone polaron states in ceria using the functionals LDA+U, GGA+U, PBE0 [11] and HSE (both HSE03 [12] and HSE06 [13]).

2. Method

We use plane-wave *ab initio* DFT with the Projector Augmented Wave method [14] (PAW) within the VASP code [15]. O$2s^2 2p^4$ and Ce$4f^1 5s^2 5p^6 5d^1 6s^2$ are treated as valence, with a plane-wave cutoff of 300 eV. We use a 96 atom supercell, which is a 2×2×2 multiple of the 12 atom crystallographic cell. K-point integrations use a 4×4×4 and 2×2×2 Monkhorst-Pack grids [16] for LDA/GGA+U and hybrid calculations respectively. We use the rotationally invariant form of LDA+U due to Dudarev et al. [17], together with LDA and with the PBE form of GGA.

3. Results

3.1. Real space charge localization with different functionals

In line with previous studies of $\left[V_O^{+2} - 2Ce_{Ce}^{-1}\right]$ complexes, we find that all the functionals studied can localize Ce*4f* electrons to form small polarons, as illustrated by the isocharge surfaces in Fig 2. These show the partial charge density of the single filled Ce*4f* state. For each functional, surfaces are shown containing 85%, 90% and 95% of the total polaron charge. Clearly, the degree of localization varies, with LDA+U producing the most localized description, closely followed by GGA+U, then the hyrbids PBE0 HSE06 and HSE03. Since the experimental evidence points to very tightly localized Ce*4f* polarons, LDA+U=6 eV seems to be the most successful functional.

In order to check the choice of U=6 eV for LDA+U, we show in Fig 3 the percentage of the supercell contained within the 90% and 95% isocharge surfaces, as a function of U. Clearly, the most localized description is indeed at U=6 eV. Fig 3 also shows the equivalent data (from [7]) for the $\left[V_O^{+2} - 2Ce_{Ce}^{-1}\right]$ complex. Although equally localized near the optimal U, the lone polaron *starts* to localize at slightly higher U values than the vacancy bound polarons. It is apparently easier to localize Ce*4f* electrons when the presence of something else (such as a vacancy) has already broken the translational symmetry of the lattice.

3.2. Calculated band energies

Fig 4 shows band energies taken from the density of states (DOS) of a supercell containing a single Ce*4f* electron, and no other defects. (c.f. schematic in Fig 1). Fig 4 (a) plots the variation of these energies with U for LDA+U. (The inset shows very similar results for GGA+U.) Once localized, the polaron state descends roughly linearly with U, falling 2.1 eV to reach the valence

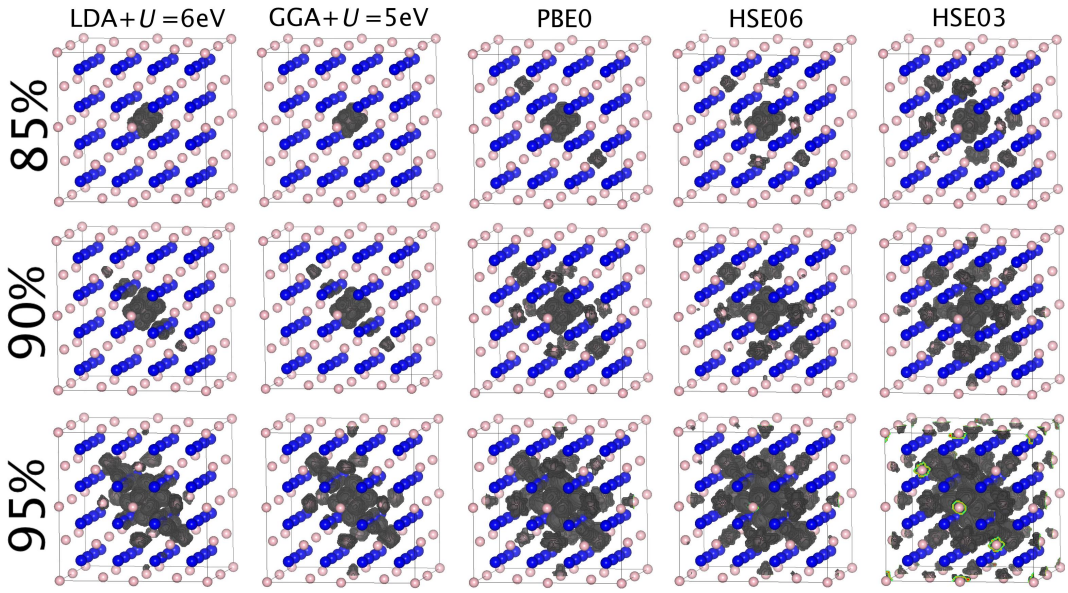

Figure 2. Isocharge surfaces containing 85%, 90% and 95% of the Ce*4f* charge, obtained using the functionals LDA+U=6 eV, GGA+U=5 eV, PBE0, HSE06 and HSE03.

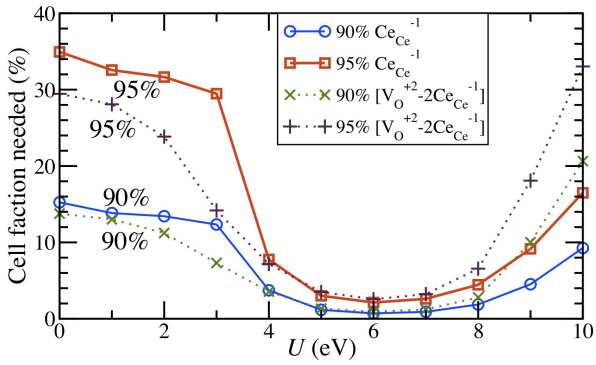

Figure 3. Volume of the supercell contained within the 90% and 95% isosurfaces of Fig 2 for the polaron (solid lines) and for the $\left[V_O^{+2} - 2Ce_{Ce}^{-1}\right]$ complex (dotted lines), as a function of U for LDA+U. Data for $\left[V_O^{+2} - 2Ce_{Ce}^{-1}\right]$ taken from [7].

band at $U \simeq 10$ eV. The effect of U on the empty states is much milder, with the Ce*4f*(empty) states rising by only 0.7 eV and the *Ce5d* states falling by 0.4 eV over the same range of U values. In other words, the improvement in the description of the polarons obtained from LDA+U and GGA+U is due primarily to the effect U has on the *filled* Ce*4f* states.

The HSE functional contains a screening range separation parameter μ. Choosing μ=0 gives the PBE0 functional, μ=0.2 gives HSE06, μ=0.3 gives HSE03 and the limit $\mu \to \infty$ recovers pure PBE. In Fig 4 (b) we show the evolution of the band positions with μ. In contrast to LDA/GGA+U, these hybrids have virtually no direct effect on the energy of the filled Ce*4f* state, at least once it has left the Ce*4f* (empty) band. Instead, the improvements are obtained by moving the *empty* states *upwards* in energy. While this is to be expected, given the nature of the hybrids, the difference between this and LDA/GGA+U is striking. Both approaches produce qualitatively reasonable results, but their detailed predictions for the properties of polarons and other features of ceria can therefore be expected to be very different indeed.

Conclusions

We have shown that, while they all correctly localize Ce*4f* electrons in ceria to form small polarons, the functionals LDA+U and GGA+U form much more tightly localized polarons than

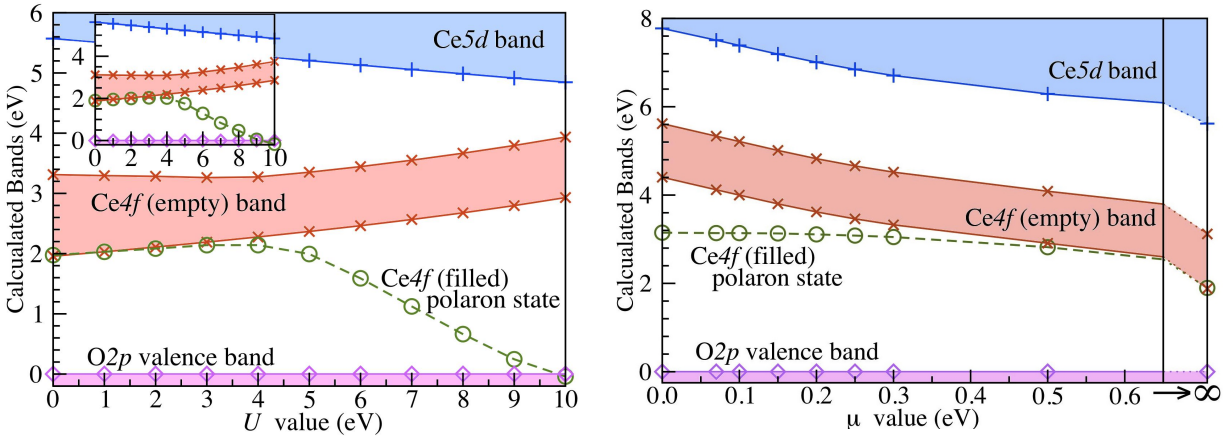

Figure 4. Bands in ceria with one filled Ce*4f* state, as a function of (a) U for LDA+U (inset: GGA+U), and (b) μ for HSE-type functionals: PBE0 ($\mu = 0$) HSE06 ($\mu = 0.2$), HSE03 ($\mu = 0.3$) and pure PBE ($\mu \to \infty$). Energies plotted relative to the valence band edge.

the hybrids PBE0, HSE06 and HSE03, and are thus more in keeping with the experimental data. We have confirmed that U=6 eV is the optimal value for describing lone polarons with LDA+U. We have also shown that the improvement in the description of polarons obtained from LDA+U and GGA+U is due primarily to the effect that U has on the *filled* Ce*4f* states, but the improvement obtained using hybrids is due primarily to their effect on the *empty* states. This difference will impact many of the detailed predictions made using the two classes of functional, and this fundamental difference in behaviour has not perhaps received the attention in the literature that it deserves.

References

[1] Esch F, Fabris S, Zhou, Montini T, Africh C, Fornasiero P, Comelli G and Rosei R, 2005 *Science* **309** 752
[2] Lu Z, Yang Z, Hermansson K and Castleton C W M 2014 *J. Mater. Chem. A* **2** 2333
[3] Tuller H L and Nowick A S 1977 *J. Phys. Chem. Solids* **38** 859
Naik I K and Tien T Y 1978 *J. Phys. Chem. Solids* **39** 311
Chang E K and Blumenthal R N 1988 *J. Sol. Stat. Chem.* **72** 330
[4] Holstein T 1959 *Ann. Phys.* **8** 325, **8** 343
[5] Kullgren J, Hermansson K, Castleton C W M, 2012 *J. Chem. Phys.* **137** 044705
[6] Hay P J, Martin R L, Uddin J and Scuseria G E 2006 *J. Chem. Phys.* **125**, 034712
Kullgren J, Castleton C W M, Müller C, Muñoz Ramo D and Hermansson K 2010 *J. Chem. Phys.* **132** 054110
[7] Castleton C W M, Kullgren J and Hermansson K 2007 *J. Chem. Phys.* **127** 244704
[8] Loschen C, Carrasco J, Neyman K N, and Illas F 2007 *Phys. Rev. B* **75** 035115
Andersson D A, Simak S I, Johansson B, Abrikosov I A, and Skorodumova N V 2007 *Phys. Rev. B* **75** 135109
[9] Da Silva J L F Ganduglia-Pirovano M V, Sauer J, Bayer V and Kresse G 2007 *Phys. Rev. B* **75** 045121
[10] Nakayama M, Ohshima H, Nogami M and Martin M 2012 *Phys. Chem. Chem. Phys.* **14** 6079
Zacherle T, Schriever A, De Souza R A and Martin M 2013 *Phys. Rev. B* **87** 134104
Plata J J, Marquez A M, and Sanz J F. 2013 *J. Phys. Chem. C*, 2013 **117** 14502
Plata J J, Marquez A M, and Sanz J F. 2013 *J. Phys. Chem. C*, 2013 **117** 25497
[11] Adamo C and Barone V 1999 *J. Chem. Phys.* **110** 6158
[12] Heyd J, Scuseria G E and Ernzerhof M 2003 *J. Chem. Phys.* **118** 8207
[13] Heyd J, Scuseria G E and Ernzerhof M 2006 *J. Chem. Phys.* **124** 219906
[14] Blöchl P E, Phys. 1994 *Phys. Rev. B* **50** 17953
Kresse G and Joubert D 1999 *Phys. Rev. B* **59** 1758
[15] Kresse G and Furthmüller J 1996 *Comp. Mat. Sci.* **6** 15
[16] Monkhorst H and Pack P 1976 *Phys. Rev. B* **13** 5188
[17] Dudarev S L, Botton G A, Savrasov S Y, Humphreys C J and Sutton A P 1998 *Phys. Rev. B* **57** 1505